1975ICRC....1..263L

COMPOSITION CHANGES IN THE IRON GROUP BETWEEN 0.5 AND 10 GeV/n

N. Lund, I.L. Rasmussen, B. Peters
M. Rotenberg, N.J. Westergaard

Danish Space Research Institute
Lundtoftevej 7, 2800 Lyngby, Denmark

Data from a recent balloon flight show that the abundance of nickel is increasing relative to the abundance of iron at energies of a few GeV/n. As there is no appreciable spallation contribution to either iron or nickel the observed effect can not be explained as a propagation effect but must be an indication of contribution from different sources.

I. Introduction

In a 60 hour balloon flight carried out in September 1974 from Sioux City, Iowa, we measured the chemical composition of primary cosmic ray nuclei at kinetic energies above 500 MeV/n. We present here preliminary findings concerning the composition for the elements above Silicon. We discuss briefly the calibration procedure and some residual bias in our data caused by the data selection procedures. A more complete description of our instrumentation will be published in a forthcoming paper.

II. Instrumentation and Calibration

Our instrument consists of four white diffusing counter boxes with Cerenkov- and scintillation radiators and a neon flash tube hodoscope. The arrangement of the radiators can be seen from Fig. 1. (See ref. 1 for a description of the aerogel radiator).

The uniformity of the counters is such that we can identify the carbon and oxygen nuclei in the raw data. We then use these nuclei to construct calibration maps for the variation in the light collection over the radiator surfaces.

For the two PVT radiators (see Fig. 1) the calibration work has been complicated because the correction map turned out to be slightly charge dependent. This is probably related to the rather strong scintillation component present in this material. For the light elements the scintillation dominated over the Cerenkov emission even for relativistic particles. In the iron group the situation was reversed because of the nonlinearity of the scintillation response. Apparently the calibration map determined from carbon and oxygen, where the scintillation was strong, did not

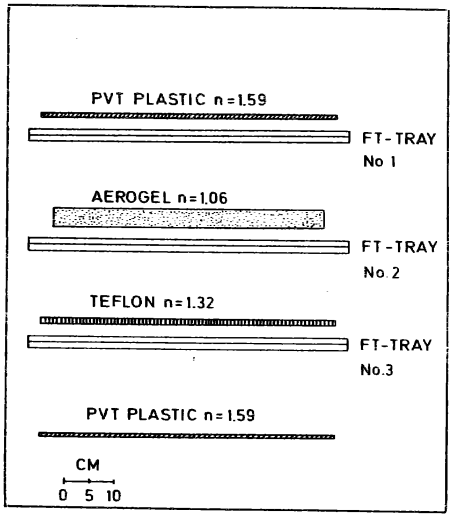

Fig. 1
Detector layout
Geometric factor = 770 cm^2 sterad

© MPE • Provided by the NASA Astrophysics Data System

1975ICRC....1..263L

coincide with the map relevant for iron nuclei where the Cerenkov emission dominated. In order to determine the additional corrections required for the higher charges we used high energy iron nuclei selected on the basis of the signals from the teflon and the aerogel counters. (In these counters, because of the absence of a scintillation component, the same map applies to all charges).

The final resolution we have obtained in the iron group can be judged from Fig. 2, it is not as good as we have obtained in earlier flights using F2 lead glass in place of the PVT.

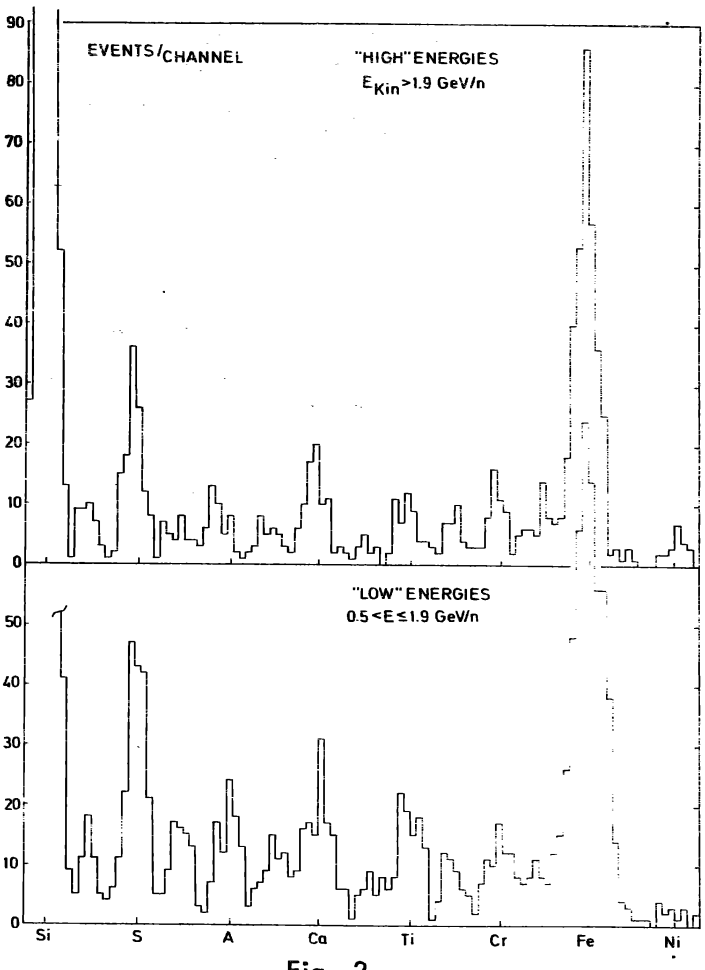

Fig. 2
Charge histograms for the two energy ranges. The data shown are uncorrected for nuclear interactions in the instrument or the overlying atmosphere.

III. Residual Bias in the Data

The data which are presented here have not yet been corrected for some charge and energy dependent bias arising from the use of a neon flash hodoscope. The hodoscope consists of 3 trays with layers in the X and the Y direction. In the computer analysis of the events a search is made for straight lines defined by a group of flashes in each tray. If one and only one such line is found (in both X and Y) the event is accepted, otherwise it is rejected. Obviously the probability of finding a unique line depends on the average number of discharged tubes per event. It is difficult to control very accurately this number over a wide range of specific ionizations and in a heavy background of fast knock-on electrons. We have employed in the balloon instrument an active control circuit which for each particle adjusts the delay in the firing of the high voltage pulser according to the signal in the top PVT counter. In this way we have succeeded to compensate quite well for the variation in specific ionization with particle charge. But the variation of the number of knock-on electrons with energy for each charge still causes a moderate increase in the number of flashing tubes with increasing particle energy.

We estimate that in the energy range above 1.9 GeV/n the straight line algorithm used have rejected less than 10% of the carbon nuclei and less than 25% of the iron group nuclei. The resulting loss of particles is a smoothly increasing function

© MPE • Provided by the NASA Astrophysics Data System

1975ICRC....1..263L

of the particle energy and is changing by less than 1% between neighboring elements.

IV. Results

The measured abundances corrected for the interactions in the instrument and in the 4 g/cm^2 of overlying atmosphere is given in table I.

The division between the two energy ranges in the table is determined by the Cerenkov threshold of the aerogel radiator at 1.9 GeV/n kinetic energy. Below this energy the charge is determined by the PVT counter signals with a small energy correction derived from the teflon counter signal. Above 1.9 GeV/n both the PVT and the teflon signals are used to determine the charge, the energy correction is provided by the aerogel signal. The latter procedure provides a more precise charge determination which can be seen from Fig. 3 where the iron peak region is shown in bi-dimensional form.

TABLE I

OBSERVED EVENTS AND ABUNDANCES RELATIVE TO IRON

Z	Events ± uncertainty[1]		Ratios at top of atmosphere	
	0.5< E< 1.9	E≥ 1.9 GeV/n[2]	0.7< E< 2.1	E≥ 2.1 GeV/n
14	1030 ± 32	707 ± 26	1.66 ± 0.07	1.65 ± 0.07
15	51 ± 10	37 ± 6	0.07 ± 0.02	0.07 ± 0.02
16	203 ± 14	118 ± 11	0.32 ± 0.03	0.28 ± 0.03
17	73 ± 10	29 ± 8	0.11 ± 0.02	0.06 ± 0.02
18	102 ± 12	51 ± 8	0.17 ± 0.03	0.11 ± 0.02
19	65 ± 12	32 ± 6	0.10 ± 0.02	0.07 ± 0.02
20	132 ± 12	84 ± 9	0.23 ± 0.02	0.21 ± 0.03
21	34 ± 8	16 ± 5	0.06 ± 0.02	0.03 ± 0.01
22	98 ± 10	53 ± 8	0.17 ± 0.02	0.14 ± 0.03
23	48 ± 8	35 ± 8	0.08 ± 0.02	0.09 ± 0.02
24	79 ± 10	53 ± 10	0.14 ± 0.02	0.13 ± 0.03
25	44 ± 15	40 ± 15	0.07 ± 0.03	0.09 ± 0.04
26	485 ± 22	336 ± 18	1.0	1.0
27	-	4 ± 4	-	0.01 ± 0.01
28	17 ± 4	21 ± 5	0.04 ± 0.01	0.07 ± 0.02

[1] The uncertainty includes both statistical uncertainties and the estimated uncertainty in the charge assignment.

[2] Kinetic energy.

© MPE • Provided by the NASA Astrophysics Data System

1975ICRC....1..263L

It is evident from Fig. 3 that a change in the nickel abundance occurs around 1 GeV/n. In table II we give the iron and nickel abundances above and below 1 GeV/n at the instrument. (This corresponds to ~ 1.2 GeV/n at the top of the atmosphere).

V. Discussion

The observed change of the Ni/Fe ratio is interesting because it is unlikely to arise during acceleration and propagation. The nickel and the iron nuclei which one observes near the Earth are essentially primordial. A variation in their relative abundance with energy means then that different sources predominate at different energies.

VI. Acknowledgements

The balloon flight was part of the Saclay-Lyngby Collaboration for HEAO and was supported by the NASA HEAO project. We are indebted to our French collaborators for providing us with the Aerogel radiator and for support during the balloon campaign. We are also indebted to the NCAR launch team which put much effort into assuring the success of the flight.

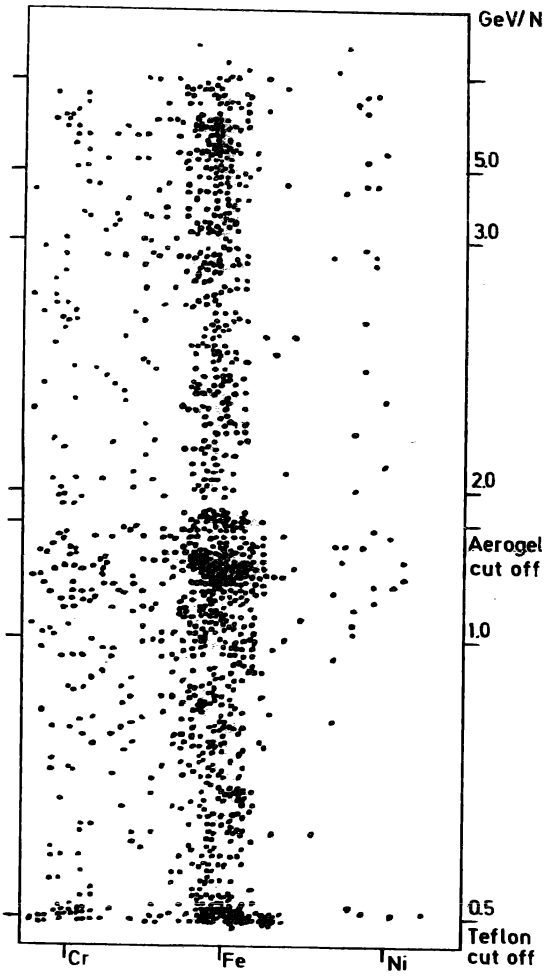

Table II

IRON AND NICKEL ABUNDANCES

	$0.7<E<1.2$	$E\geq 1.2$ GeV/n
Fe events	298	541
Ni events	6	35
Ni/Fe	0.020 ± 0.008	0.065 ± 0.011

References

1) Cantin, M., Engelman, J., Koch, L., Masse, P., Byrnak, B., and Lund, N., Paper T 2-8. This Conference.

Fig. 3 Bi-dimensional diagram showing the iron peak and the neighboring elements. The horizontal scale is a charge scale. Below 1.9 GeV/n it is based on the PVT counter signals and, for energies above 1.9 GeV/n, on the PVT and the teflon signals. The vertical scale is an energy scale, it is the sum of the Teflon and the Aerogel signals divided by the sum of the PVT signals. The scarcity of nickel below 1 GeV/n is apparent.

© MPE • Provided by the NASA Astrophysics Data System